crystals

MDPI

Article

The $Na_{2-n}H_n[Zr(Si_2O_7)]\cdot mH_2O$ Minerals and Related Compounds (n = 0–0.5; m = 0.1): Structure Refinement, Framework Topology, and Possible Na^+-Ion Migration Paths

Natalya A. Kabanova [1,2], Taras L. Panikorovskii [1,3,*], Vladimir V. Shilovskikh [4], Natalya S. Vlasenko [4], Victor N. Yakovenchuk [5], Sergey M. Aksenov [1], Vladimir N. Bocharov [4] and Sergey V. Krivovichev [3,6]

1 Laboratory of Nature-Inspired Technologies and Environmental Safety of the Arctic, Kola Science Centre, Russian Academy of Sciences, Fersmana str. 14, 184209 Apatity, Russia; n.kabanova@ksc.ru (N.A.K.); s.aksenov@ksc.ru (S.M.A.)
2 Samara Center for Theoretical Materials Science, Samara State Technical University, Molodogvardeyskaya Str. 244, 443100 Samara, Russia
3 Crystallography Department, Institute of Earth Sciences, St. Petersburg State University, University emb. 7/9, 199034 Petersburg, Russia; s.krivovichev@ksc.ru
4 Geo Environmental Centre "Geomodel", Saint–Petersburg State University, Ul'yanovskaya Str. 1, 198504 Petersburg, Russia; vova_bel@mail.ru (V.V.S.); n.vlasenko@spbu.ru (N.S.V.); bocharov@molsp.phys.spbu.ru (V.N.B.)
5 Geological Institute, Kola Science Centre, Russian Academy of Sciences, Fersmana str. 14, 184209 Apatity, Russia; v.yakovenchuk@ksc.ru
6 Nanomaterials Research Centre, Kola Science Centre, Russian Academy of Sciences, Fersmana str. 14, 184209 Apatity, Russia
* Correspondence: t.panikorovskii@ksc.ru; Tel.: +7-8155-579-628

Received: 26 October 2020; Accepted: 6 November 2020; Published: 9 November 2020

check for updates

Abstract: The $Na_{2-n}H_n[Zr(Si_2O_7)]\cdot mH_2O$ family of minerals and related compounds (n = 0–0.5; m = 0.1) consist of keldyshite, $Na_3H[Zr_2(Si_2O_7)_2]$, and parakeldyshite, $Na_2[Zr(Si_2O_7)]$, and synthetic $Na_2[Zr(Si_2O_7)]\cdot H_2O$. The crystal structures of these materials are based upon microporous heteropolyhedral frameworks formed by linkage of Si_2O_7 groups and ZrO_6 octahedra with internal channels occupied by Na^+ cations and H_2O molecules. The members of the family have been studied by the combination of theoretical (geometrical–topological analysis, Voronoi migration map calculation, structural complexity calculation), and empirical methods (single-crystal X-ray diffraction, microprobe analysis, and Raman spectroscopy for parakeldyshite). It was found that keldyshite and parakeldyshite have the same **fsh** topology, while $Na_2ZrSi_2O_7\cdot H_2O$ is different and has the **xat** topology. The microporous heteropolyhedral frameworks in these materials have a 2-D system of channels suitable for the Na^+-ion migration. The crystal structure of keldyshite can be derived from that of parakeldyshite by the $Na^+ + O^{2-} \leftrightarrow OH^- + \square$ substitution mechanism, widespread in the postcrystallization processes in hyperagpaitic rocks.

Keywords: keldyshite; parakeldyshite; crystal structure; ion migration; transformation; Raman spectroscopy; Voronoi analysis; topology

1. Introduction

Microporous zirconosilicates attract considerable interest as ionic conductors, molecular sieves, and ion exchangers [1–3]. Among them, compounds with the NASICON-type structures are considered

as ionic conductors, while sodium amphoterosilicates (e.g., ETS-4) are of interest as selective adsorbents for ^{137}Cs and ^{90}Sr radioactive isotopes [2,4–10]. The beginning of the study of zirconium silicate was stimulated by the discovery of keldyshite-group minerals in the Lovozero alkaline massif, Kola peninsula, Russia [11–15].

Keldyshite, $(Na,H)_2[Zr(Si_2O_7)]$, was discovered in 1962 and the further detailed study of its holotype material indicated the existence in the mineral sample of polysynthetic intergrowths of two phases $Na_3HZr_2(Si_2O_7)_2$ and $Na_2[Zr(Si_2O_7)]$ (renamed as keldyshite and parakeldyshite, respectively) [16]. The crystal-structure model for parakeldyshite was proposed in 1970 [17] and confirmed in 1974 [18]. The crystal structure of keldyshite was determined in 1978 [19], when the similarity between the crystal structures of keldyshite and parakeldyshite was demonstrated. The "M-34 phase" with the idealized chemical formula $NaH[Zr_2(Si_2O_7)]\cdot H_2O$ was discovered in the samples of parakeldyshite from Khibiny alkaline massif, but its crystal structure remains unknown [16].

General mineralogical and structural relationships between keldyshite, parakeldyshite, and the "M-34 phase" allowed establishment of the 'parakeldyshite → keldyshite → "M-34 phase"' transformational group of minerals (similar to the 'kazakovite → tisinalite' [20], 'zirsinalite → lovozerite' [21], etc. series). Within each group, transformation of the minerals is induced by ion-exchange reactions under natural conditions [22–26].

Synthetic zirconium silicates related to keldyshite are known [5,6] and can be obtained by different methods: (i) by crystallization from a melt at the temperature range 1000–1250 °C or (ii) by the hydrothermal technique at the temperatures of 450–500 °C [1,3]. Recently, an alternative model of the arrangement of Na cations in parakeldyshite was obtained [27] and the phase $Na_2ZrSi_2O_7\cdot H_2O$ was discovered, which is close in composition to the M-34 phase [28]. Keldyshite-related compounds have serious potential for their use in the purification of gases from sulfur dioxide in the production of sulfuric acid and heavy non-ferrous metals from sulfide ores [29]. Further work determined the presence of ion-exchange properties in the new zirconosilicate minerals discovered on the territory of the Kola alkaline province [27,30–32].

In this paper, we report the results of the theoretical analysis of the Na^+-ion migration paths in the crystal structures of keldyshite, parakeldyshite, and zirconium silicate $Na_2[Zr(Si_2O_7)]\cdot H_2O$ using a geometrical and topological approach [33,34]. The crystal structure of parakeldyshite was refined using the sample from albitized pegmatite at Takhtarvumchorr Mt., Khibiny alkaline massif, Russia. The transformational nature of keldyshite-related minerals is discussed.

2. Materials and Methods

2.1. Sample

A sample of parakeldyshite was collected from albitized pegmatites at the Takhtarvumchorr Mt. (Khibiny massif). Albitites are composed of a fine-fine-grained aggregate of lamellar albite with lenses (up to 1 × 0.5 m) of sugar-like apatite. The mass contains flattened prismatic crystals of enigmatite, flakes and radial-radiant aggregates of molybdenite, plates of ilmenite and pyrrhotite, and dark-orange prismatic spherulites of pale cream fibrous chirvinskyite. Parakeldyshite was found as transparent barley-like crystals up to 2 mm long, with the marginal zones replaced by powdery precipitates of the "M-34 phase" [22] with the chemical composition $NaH[Zr(Si_2O_7)]$ (Figure 1). In association with parakeldyshite, spherulites of chirvinskyite, lemon-yellow radial-radial aggregates, and individual prismatic crystals of titanite (partially replaced by lorenzenite, eudialyte, and zircon grains) have been observed.

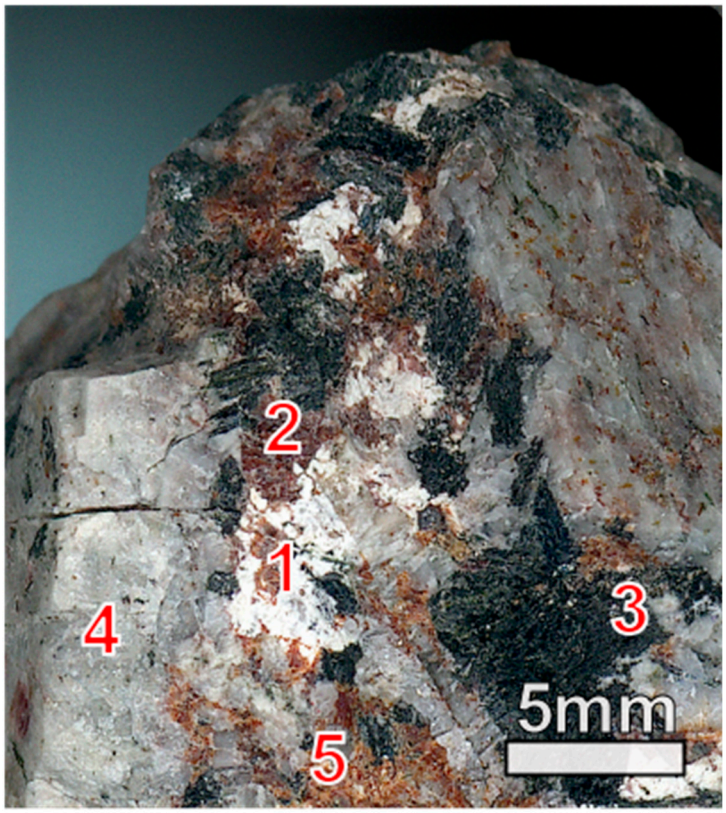

Figure 1. Powdered aggregates of parakeldyshite/keldyshite (1) in association with eudialyte (2), aegirine (3), albite (4), and låvenite (5) in albitized pegmatite in foyaites at Takhtarvumchorr Mt.

2.2. Composition

The chemical composition of parakeldyshite was determined at the 'Geomodel' resource center of St. Petersburg State University using the scanning electron microscope Hitachi S-3400N equipped by INCA 500 WDS detector operating at 20–30 nA and 20 kV. The analyses were performed with the beam size of 5 µm and the counting time of 10–20/10 s on peaks/background for each chemical element. Quartz (Si), corundum (Al), calcite (Ca), halite (Na), zircon (Zr), rutile (Ti), hematite (Fe), celestine (Sr), and rhodonite (Mn) were used as standards. An average chemical composition based on 5 analyzes (in wt.%): ZrO_2 39.95, Na_2O 20.02 SiO_2 39.41, sum 99.38 The empirical formula calculated per 5 cations can be written as: $Na_{1.99}Zr_{0.99}Si_{2.02}O_{7.015}$.

2.3. Single-Crystal X-ray Diffraction

The crystal-structure studies of parakeldyshite were carried out at the X-ray Diffraction Resource Centre of St. Petersburg State University on an Agilent Technologies Xcalibur EOS diffractometer equipped with the CCD detector using monochromatic Mo$K\alpha$ radiation (λ = 0.71069 Å) at room temperature. More than a hemisphere of diffraction data was collected (scanning step 1°, exposure time 10 s). The absorption correction was done empirically using spherical harmonics implemented in the SCALE ABSPACK calibration algorithm in the CrysAlysPro software package [35]. The unit-cell parameters were determined and refined by the least squares method using 1364 independent reflections. The structure was refined using the SHELXL software package [36]. The data are deposited in CCDC under Entry No. 22040710. The coordination number of Na determined by number bonds with maximal length constrained 3.10 Å. Crystal data, data collection information, and refinement details are given in Table 1. Atom coordinates and isotropic parameters of atomic displacements are given in Table S1, interatomic distances in Table S2, and the anisotropic parameters of atomic displacements are given in Table S3.

Table 1. Crystal data, data collection information, and refinement details for parakeldyshite from Takhtarvumchorr Mt., Khibiny, Russia.

Parameter	Data
Temperature/K	293(2)
Crystal system	triclinic
Space group	$P\bar{1}$
a/Å	5.4243(6)
b/Å	6.5923(5)
c/Å	8.8083(6)
α/°	71.309(7)
β/°	87.162(8)
γ/°	85.497(8)
Volume/Å^3	297.34(5)
Z	2
ρ_{calc}/g cm^{-3}	3.411
μ/mm^{-1}	2.388
F(000)	292.0
Crystal size/mm^3	0.17 × 0.12 × 0.11
Radiation	Mo *K*α (λ = 0.71073)
2θ range for data collection/°	6.538 to 54.986
Index ranges	$-5 \leq h \leq 7$, $-8 \leq k \leq 8$, $-11 \leq l \leq 10$
Reflections collected	2296
Independent reflections	1364 [R_{int} = 0.0221, R_σ = 0.0362]
Data/restraints/parameters	1364/0/109
Goodness-of-fit on F^2	1.120
Final *R* indexes [$I \geq 2\sigma(I)$]	R_1 = 0.0237, wR_2 = 0.0602
Final R indexes [all data]	R_1 = 0.0256, wR_2 = 0.0616
Largest diff. peak/hole/*e* Å^{-3}	0.79/−0.69

2.4. Geometrical–Topological Analysis

Geometrical–topological analysis of the crystal structures of keldyshite-related compounds was carried out using algorithms implemented in the ToposPro software package (https://topospro.com/) [33]. Maps of the migration of Na^+-ions were constructed by the Voronoi method, which was shown to be efficient for various types of ionic conductors [34,37,38]. The radius of an elementary channel (R_{chan}) suitable for Na^+-ion migration was chosen as 2.0 Å, similar to that reported previously [38,39].

Topological analysis of the crystal structures of keldyshite-related compounds also included the determination of the type basic grid, the construction of tiling, and the search for topologically similar inorganic compounds. The base grid is a graph whose vertices are the centers of gravity of the structural units, i.e., SiO_4 tetrahedra and ZrO_6 octahedra [40]. After contraction of doubly connected nodes ("bridging" oxygen atoms), a 4,6-coordinated grid was obtained (Figure 2).

The topological classification of the atomic nets in crystal structures was carried out in accordance with the following basic principle [41]: atomic nets with the same set of topological indices (coordination sequence, vertex symbols) belong to the same topological type [42]. In the case of the presence of stable polyhedral units in the crystal structure, the classification was carried out according to the basic grid [40]. Determination of the topological mesh type was performed using the ToposPro complex of the TopCryst web service (http://topcryst.com), which contains data on about 190,000 topological types of the nets.

The tiling theory, which is actively used to study and analyze the crystal structures of zeolites [43] and zeolite-related materials with heteropolyhedral frameworks [44–46], was introduced and developed by M. O'Keeffe [47]. This approach allows study of the smallest cavities in inorganic frameworks that can be used to fill the entire crystal space [47]. Since the grids in the crystal structures of keldyshite and parakeldyshite have the same topology, the set of tilings in these structures is the same.

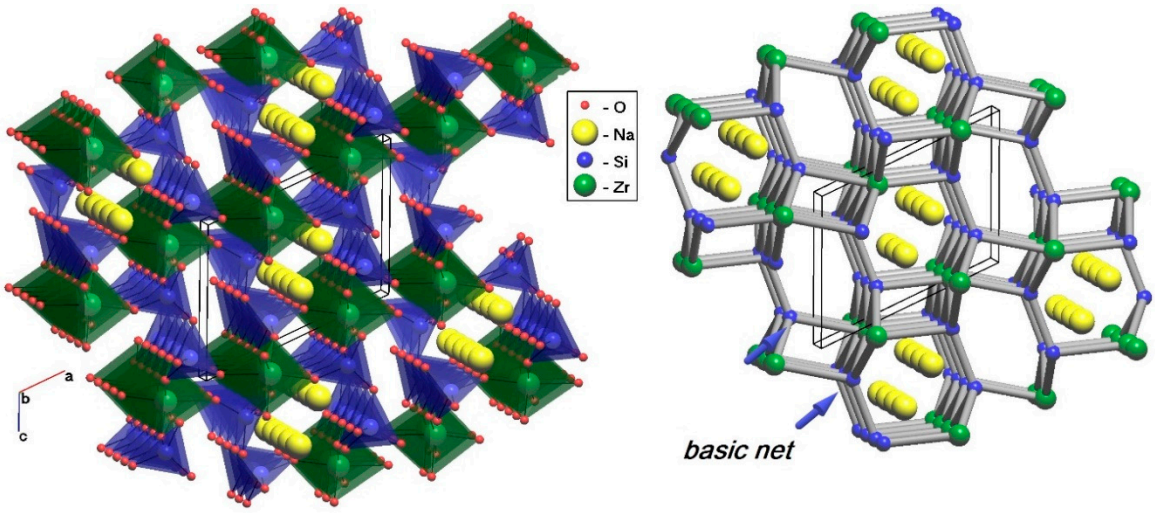

Figure 2. Basic net representation for the crystal structure of keldyshite.

2.5. Raman Spectroscopy

The Raman spectrum (RS) was obtained using a Horiba Jobin-Yvon LabRam HR 800 spectrometer (Geomodel Resource Center, St. Petersburg State University) from the surface of a parakeldyshite crystal at room temperature and a wavelength of 514 nm in the range from 4000 to 80 cm^{-1}. The baseline correction was carried out using the algorithms implemented in the OriginPro 8.1 software package.

3. Results

3.1. Single-Crystal X-ray Diffraction

The crystal structures of microporous zirconium silicates are based upon frameworks consisting of ZrO_6 octahedra and SiO_4 tetrahedra linked via common O atoms. According to the structural classification proposed by Ilyushin and Blatov [40], the crystal structures of keldyshite, $NaH[Zr(Si_2O_7)]$, parakeldyshite, $Na_2[Zr(Si_2O_7)]$, and $Na_2[Zr(Si_2O_7)]\cdot H_2O$ contain polyhedral microensembles (PME) MT_6 of the A-1 type (Figure 3).

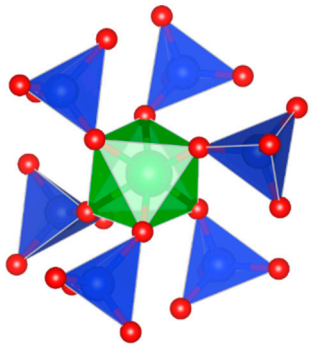

Figure 3. Polyhedral microensemble of MT_6-type forms the frameworks in the crystal structures of parakeldyshite, keldyshite, and the phase $Na_2[Zr(Si_2O_7)]\cdot H_2O$.

In the terms proposed in [5], the crystal structure of parakeldyshite can be described as a framework consisting of the M_2T_4-type secondary building units (SBUs) with Na atoms in adjacent cavities (Figure 4a). Each ZrO_6 octahedron is linked to six SiO_4 tetrahedra, which in turn are linked to two Zr octahedra each.

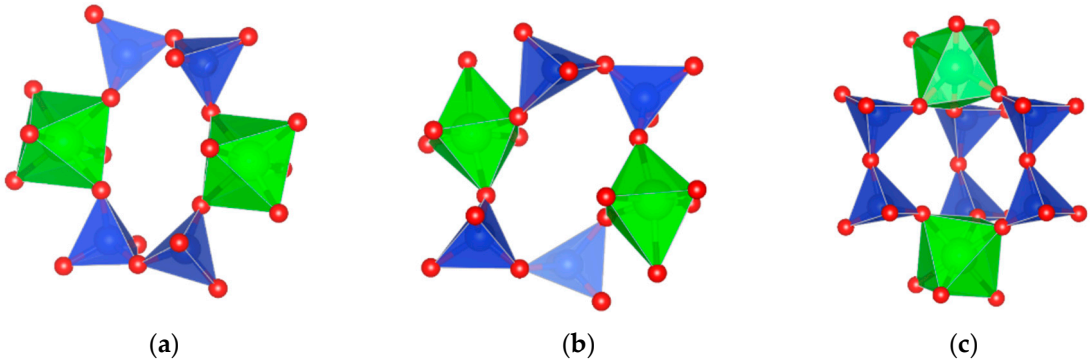

Figure 4. Secondary building units (SBUs) in Na-zirconosilicates: (**a**) M_2T_4-block in the crystal structure of parakeldyshite; (**b**) M_2T_4-block in the crystal structure of keldyshite; (**c**) M_2T_6-block in the crystal structure of the $Na_2ZrSi_2O_7$ H_2O phase.

The crystal structure of parakeldyshite from albitized pegmatite of Takhtarvumvorr Mt., Khibiny, Russia was solved in the space group $P\bar{1}$ and refined to final R_1 = 0.024 [for 1364 $F^2 > 4\sigma(F^2)$]. In general, the structure model proposed in [17] was confirmed. The bond lengths in polyhedra vary significantly and are equal to 2.047-2.139(2), 1.601-1.672(2), 1.600-1.669(2), 2.443-2.913(3), and 2.384-2.913(3) Å for the ZrO_6, $Si1O_4$, $Si2O_4$, $Na1O_8$, and $Na2O_7$ polyhedra, respectively. The degrees of distortion of polyhedra (based on bond lengths) calculated according to Baur [48] for the $Si1O_4$, $Si2O_4$, ZrO_6, $Na1O_8$, and $Na2O_7$ polyhedra are equal to 0.01369, 0.01171, 0.01626, 0.04376, and 0.07001, respectively. According to our data, there are no additional Na sites described in [27]. In contrast to keldyshite, there are two independent positions of Na1 and Na2 with a coordination number (CN) of 8, respectively, in the crystal structure of parakeldyshite (Figure 5a).

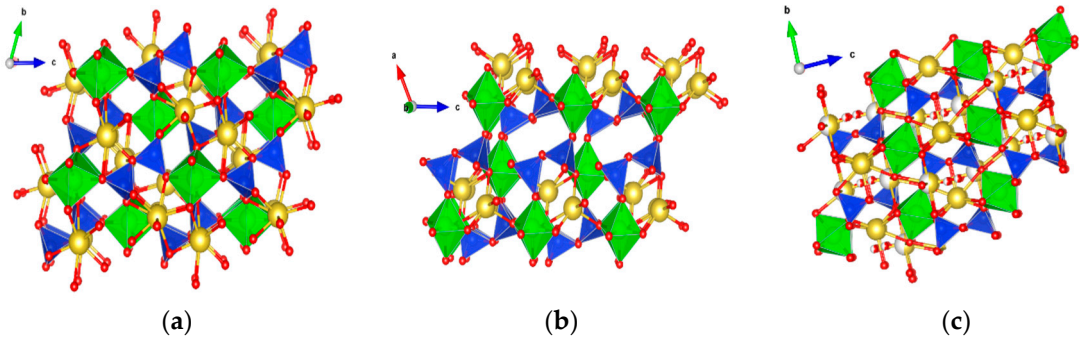

Figure 5. Projections of the crystal structures of (**a**) parakeldyshite; (**b**) keldyshite (**c**) $Na_2[Zr(Si_2O_7)]\cdot H_2O$. The SiO_4 tetrahedra are blue, the ZrO_6 octahedra are green, the Na atoms are yellow, and the O atoms are red.

The crystal structure of keldyshite (Figure 5b) differs from that of parakeldyshite and contains only one independent Na site with sevenfold coordination. The uneven distribution of Na in keldyshite results in the slight framework deformation manifested by the change of the Si–O–Si angle of 126.7(9)° compared to 127.7(8)° in parakeldyshite. At the same time, the shape of the channels changes significantly as can be clearly seen in the projection of the *MT* layer (Figure 6b).

The crystal structure of $Na_2[Zr(Si_2O_7)]\cdot H_2O$ is based on the M_2T_6 type of SBUs (Figure 4c). As in the structures of keldyshite and parakeldyshite, the ZrO_6 octahedron is linked through common vertices to six SiO_4 tetrahedra, each connected to three Zr-centered octahedra. The topological difference of the *MT*-framework (Figure 5c) from those observed in keldyshite and parakeldyshite is confirmed by the different value of the Si-O-Si angle equal to 156.96(9)°. The increasing Si-O-Si angle corresponds to the increasing size of the structure channels (Figure 6c,f).

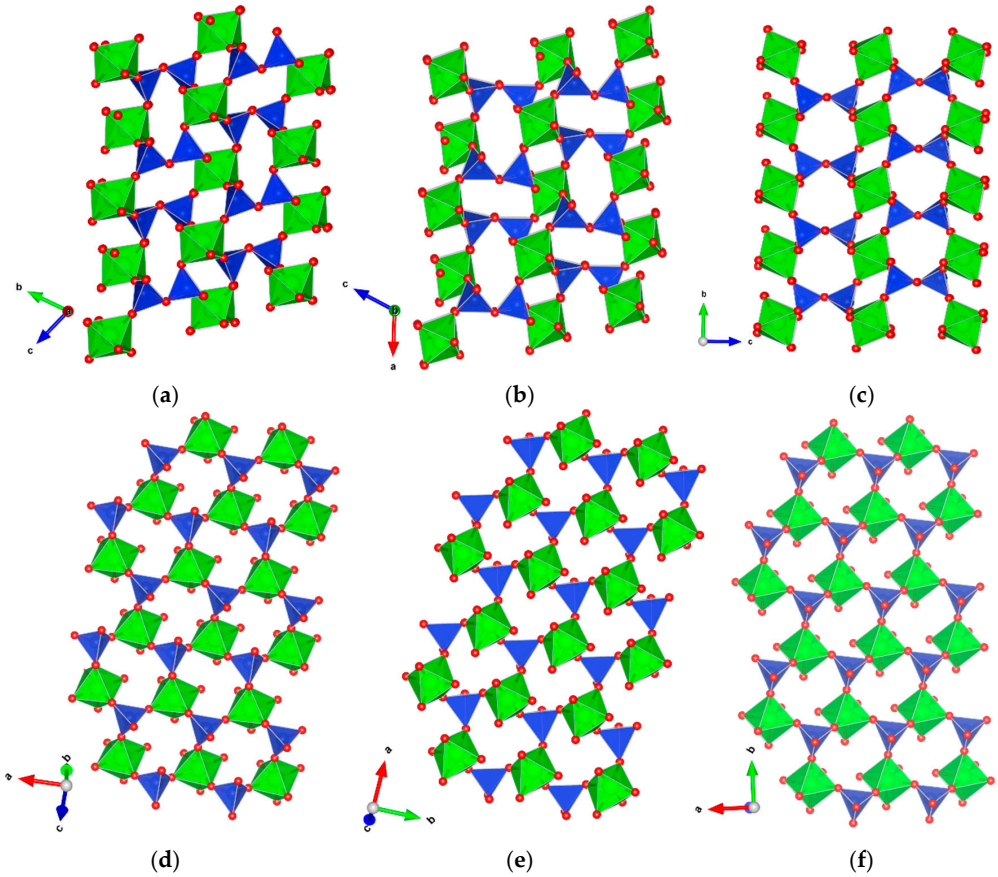

Figure 6. Projections of the *MT* layers in the crystal structures of (**a**,**d**) parakeldyshite; (**b**,**e**) keldyshite; (**c**,**f**) $Na_2[Zr(Si_2O_7)]\cdot H_2O$.

3.2. Topological Analysis

The topological type of the base grid in the crystal structures of keldyshite and parakeldyshite is **fsh**, while that in $Na_2[Zr(Si_2O_7)]\cdot H_2O$ is **xat** (Figure 7). Table 2 shows data on related inorganic compounds of the **fsh** and **xat** topological types. Keldyshite and parakeldyshite consists of one type of the $[4^3.6^3]$ tiles formed by three four-membered rings and three six-membered rings (Figure 8). In the case of $Na_2[Zr(Si_2O_7)]\cdot H_2O$, there are two types of tiles: $[6^3]$ **t-kah** and $[4^6.6^3]$ **t-afo** (Figure 8). Na atoms are located inside all $[4^3.6^3]$ tiles in parakeldyshite and only half of these tiles are filled in keldyshite. In the crystal structure of $Na_2[Zr(Si_2O_7)]\cdot H_2O$, one Na site is located in the **t-kah** tile, whereas another one is within the **t-afo** tile.

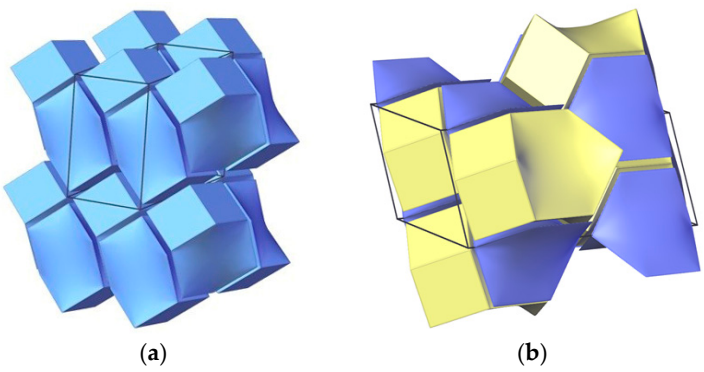

Figure 7. Tiling representation of the crystal structures of: (**a**) parakeldyshite/keldyshite (the **fsh** topology); (**b**) phase $Na_2[Zr(Si_2O_7)]\cdot H_2O$ (the **xat** topology). The $[4^3.6^3]$ tiles are shown as light-blue, the **t-afo** and **t-kah** tiles in (**b**) are yellow and violet, respectively.

Table 2. Examples of inorganic compounds with the grids of the **fsh** or **xat** topological type.

Formula	Space Group	Topology	ICSD Code	Ref.
$NaH[Zr(Si_2O_7)]$ keldyshite	$P\bar{1}$	**fsh**	20186	[47]
$Na_2[Zr(Si_2O_7)]$ parakeldyshite	$P\bar{1}$	**fsh**	–	This work
$K_2[Zr(Si_2O_7)]$ khibinskite	$P2_1/b$	**fsh**	20100	[49]
$K_2[Zr(Ge_2O_7)]$	$C2/c$	**fsh**	88843	[50]
$K_2[Cd(P_2O_7)]$	$C2/c$	**fsh**	12117	[51]
$Na[Ti(P_2O_7)]$	$P2_1/c$	**fsh**	202751	[52]
$Na_2[Si^{VI}(Si^{IV}{}_2O_7)$	$C2/c$	**fsh**	81134	[53]
$Na_2[Zr(Si_2O_7)]\cdot H_2O$	$C2/c$	**xat**	419420	[28]
$K[Y(P_2O_7)]$	$Cmcm$	**xat**	75171	[54]
$Ba_6Dy_2Al_4O_{15}$	$Cmcm$	**xat**	85071	[55]
$Si(P_2O_7)$	$P6_3$	**xat**	75116	[56]
$Tm(BO_3)$	$P\bar{6}c2$	**xat**	27942	[57]
$Na_3[Sc(Si_2O_7)]$	$Pbnm$	**xat**	20120	[58]

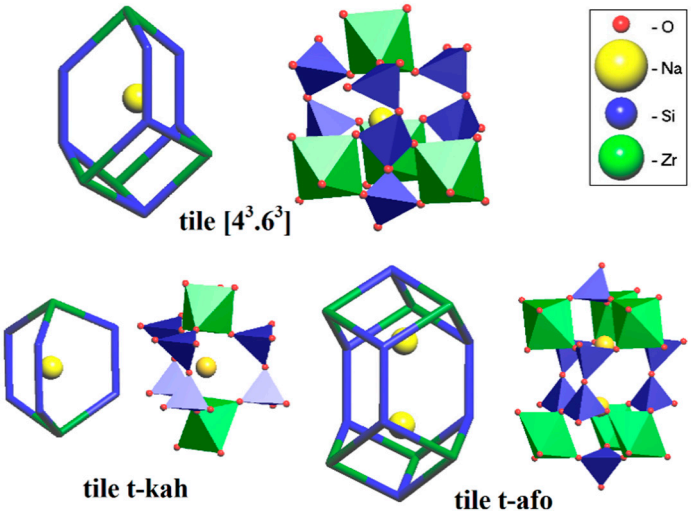

Figure 8. Fragments of the crystal structures and the corresponding tiles. The $[4^3.6^3]$ tile is present in the crystal structures of keldyshite and parakeldyshite, while the **t-kah** and **t-afo** tiles are present in $Na_2[Zr(Si_2O_7)]\cdot H_2O$.

3.3. Raman Spectroscopy

The Raman spectrum of parakeldyshite from the albitites of Takhtarvumchorr Mt. is shown in (Figure 9). The most intense spectral lines are similar to those for parakeldyshite from the Alluaiv Mt., Lovozero alkaline massif [52], RRUF, 120048 [59]. The bands in the range 850–1020 cm^{-1} correspond to stretching vibrations of Si-O bonds. Two intense absorption bands at 968 and 1017 cm^{-1} are attributed to asymmetric stretching vibrations of Si-O-Si bonds, while three bands at 850, 905, and 941 cm^{-1} are attributed to symmetric vibration modes of similar bonds [60–62]. The non-typical band at 718 cm^{-1} can be associated with symmetric stretching vibrations of the Si-O-Si bridging oxygen in sorosilicate groups [63]. The bands in the range 450–600 cm^{-1} correspond to asymmetric bending vibrations of Si-O bonds in tetrahedra [62]. Bands of different intensities in the region 350–450 cm^{-1} belong to symmetric deformation vibration modes in SiO_4 tetrahedra [63]. The most intense absorption band at 331 cm^{-1} is attributed to bending vibration modes of the Zr-O bonds in octahedra, and the bands in the range 90–300 cm^{-1} correspond to symmetric bending vibrations of bonds in octahedra or translational

vibrations [64]. The absence of bands in the region 3000–3800 cm^{-1} (Figure S1) indicates the absence of OH groups in the structure of parakeldyshite, confirming its unchanged nature.

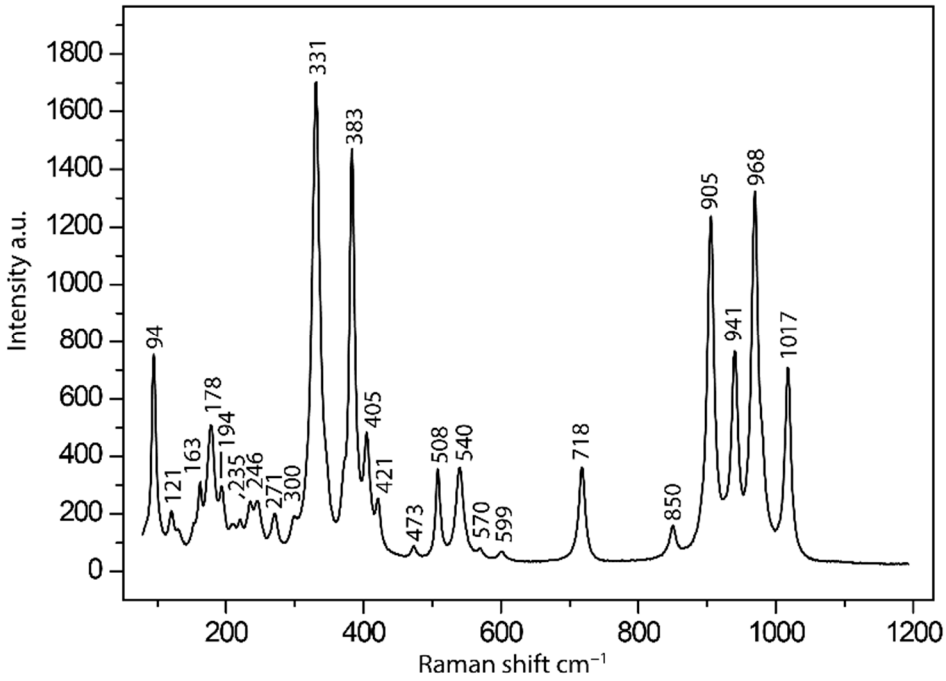

Figure 9. Raman spectrum of parakeldyshite from Takhtarvumchorr Mt., Khibiny, Russia.

4. Discussion

According to the approach of matrix (self)assembly of the crystal structures from SBUs proposed by Ilyushin for sodium zirconium silicates, all possible SBUs variants are defined as M_2T_n (n = 2, 4, 6) [5]. The crystal structure of keldyshite/parakeldyshite is based upon the M_2T_4 blocks, while the structure of $Na_2[Zr(Si_2O_7)]\cdot H_2O$ is based upon the M_2T_6 blocks. This fact indicates different formation conditions and the impossibility of the transformation of one structure type into another through the rearrangement of Na^+-ions. Indeed, the conditions of the formation of phases in the Na_2CO_3-ZrO_2-SiO_2-H_2O hydrothermal system are different: parakeldyshite crystallizes at 450 °C [5], while the $Na_2[Zr(Si_2O_7)]\cdot H_2O$ phase appears at a temperature of about 200 °C [28]. According to [65], keldyshite is a product of the sequential transformation of parakeldyshite under hypergenic conditions with the preservation of the overall framework topology. According to our data on the migration of Na^+-ions, such transition is possible.

The unit-cell parameters (Table 3) of keldyshite and parakeldeshite are close to each other and differ from those of $Na_2[Zr(Si_2O_7)]\cdot H_2O$.

Table 3. Unit cell parameters of Na-zirconosilicates chemically close to keldyshite.

Compound	Sp. Gr., Z	Unit Cell Parameters			V, Å^3	Citation
		a, Å, α, °	b, Å, β °	c, Å, γ, °		
Keldyshite $NaH[Zr(Si_2O_7)]$	$P\bar{1}$, 2	*9.01* *92.1*	*5.34* 116.1	*6.96* 88.1	300.39	[19]
Parakeldyshite $Na_2[Zr(Si_2O_7)]$	$P\bar{1}$, 2	*8.8083* *87.162*	*5.4243* 85.497	*6.5923* 71.309	297.34	Current work
$Na_2[Zr(Si_2O_7)]\cdot H_2O$	$C2/c$, 4	*10.422* *90*	*8.247* 116.55	*9.205* 90	672.2	[27]

Note. For parakeldyshite, the same setting as in the initial study of keldyshite was used (associated with that given in this work by the transition matrix 0 1 0/0 0 1/1 0 0).

The paths of the Na^+-ion migration obtained using the Voronoi method are two-dimensional, running through all the crystallographic positions of Na (Figure 10). Thus, the migration of Na^+-ions in the keldyshite-related zirconium silicates occurs along a two-periodic network of channels. Diffusion is possible when Na^+-ions move from cavity to cavity (from one tile to another) through four-membered and six-membered rings. Calculating the radius of these rings (Table 4) and comparing it with the threshold value of 2.0 Å, we can conclude that free migration of Na^+ in these structures will occur only through six-membered rings. Moreover, in the case of parakeldyshite, there is one six-membered ring that is too narrow (marked in red in Table 4) for sodium to move along. However, the migration paths through the remaining six-membered rings form a 2-D migration map, which is consistent with the result obtained by the Voronoi method.

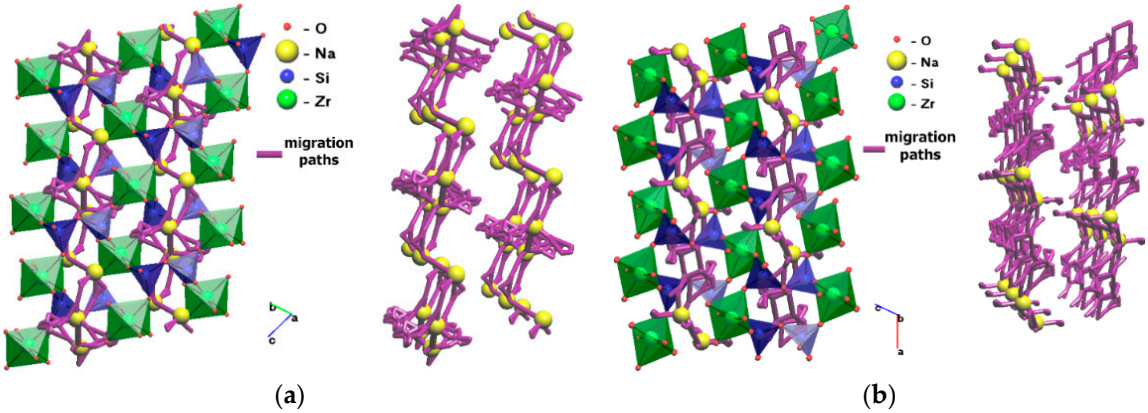

Figure 10. Migration paths of Na^+ cations obtained using the Voronoi method for the structures: (**a**) parakeldyshite; (**b**) keldyshite.

Table 4. The radii of the rings for the possible migration of Na^+ cations in the structures of keldyshite, parakeldyshite, and $Na_2ZrSi_2O_7{\cdot}H_2O$ calculated using the geometric-topological approach.

Compound	Number of Nodes in the Ring	Radius of Ring, Å	Compound	Number of Nodes in the Ring	Radius of Ring, Å
Parakeldyshite $Na_2ZrSi_2O_7$	6	2.12	Keldyshite $NaZr(Si_2O_6OH)$	6	2.09
	6	2.06		6	2.00
	6	1.75		6	2.05
	6	2.14		6	2.12
	6	2.06		6	2.10
	4	1.53		4	1.77
	4	1.54		4	1.37
	4	1.80		4	1.65
	4	1.66		4	1.84
	4	1.64		4	1.17
$Na_2ZrSi_2O_7{\cdot}H_2O$	6	2.36		4	1.77
	6	2.37		4	1.78
	4	1.75			

The refinement of the crystal structure of parakeldyshite from the Takhtarvumchorr pegmatite demonstrates the absence of splitting of the Na sites. According to the chemical data and Raman spectroscopy, the studied sample of parakeldyshite is the extreme Na-member of the possible keldyshite-parakeldyshite series. The migration paths analysis by the Voronoi method showed that all three studied phases have a 2-D system of channels (Figures 10 and 11), within which the migration of Na^+ cations is possible. These data confirm the possibility of transition from

parakeldyshite to keldyshite by the $Na^+ + O^{2-} \leftrightarrow OH^- + \square$ substitution scheme, which is widespread in postcrystallization processes in peralkaline rocks.

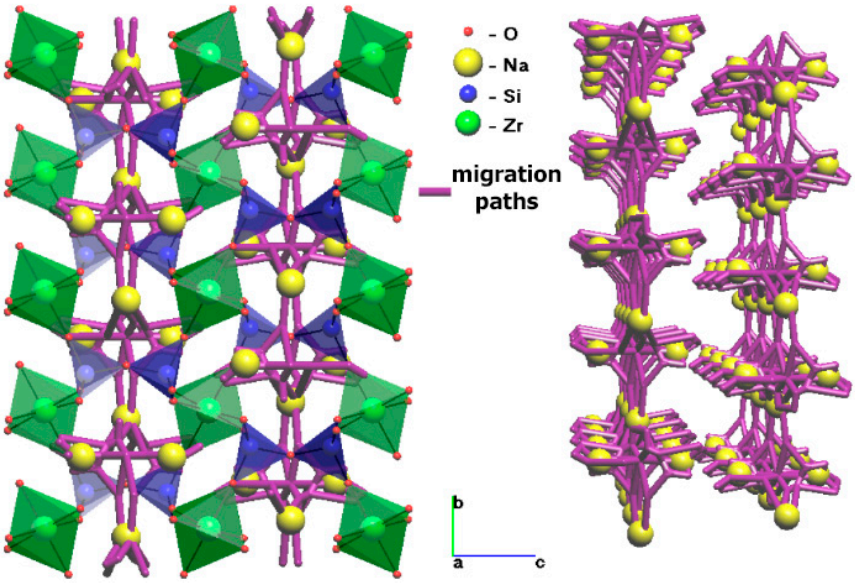

Figure 11. Migration paths of Na^+ cations obtained using the Voronoi method for the crystal structure of $Na_2[Zr(Si_2O_7)]\cdot H_2O$.

The structural complexity $I_{G,total}$ was calculated according to the method proposed in [66]. The calculated values for keldyshite/parakeldyshite and $Na_2ZrSi_2O_7\cdot H_2O$ are 76.107 and 86.606 (bits/u.c.), respectively. The identity of the structural complexity values for keldyshite and parakeldyshite emphasizes their structural similarity. The increase in structural complexity with the decreasing crystallization temperature is in agreement with the general tendency observed for hydrothermal systems [66,67].

Supplementary Materials: The following materials are available online at http://www.mdpi.com/2073-4352/10/11/1016/s1, Figure S1: title, Table S1: Fractional atomic coordinates ($\times 10^4$) and equivalent isotropic displacement parameters ($Å^2 \times 10^3$) for parakeldyshite. Table S2: selected interatomic distances in parakeldyshite. Table S3: anisotropic parameters of atomic displacements in parakeldyshite.

Author Contributions: N.A.K. and T.L.P. designed the study. V.V.S. and N.S.V. performed microprobe analyses, V.N.Y. provide samples for investigation. V.N.B. performed Raman spectroscopy measurements, T.L.P. performed and interpreted Single-crystal X-ray diffraction experiments. N.A.K., T.L.P. and S.M.A. wrote the draft paper. S.V.K. supervising, review and editing. All authors have read and agreed to the published version of the manuscript.

Funding: This work was supported by the Kola Science Center of Russian Academy of Sciences (Project 0226-2019-0011) and funded by the Russian Foundation for Basic Research (Grant 18-29-12039). N.A.K. thanks the Ministry of Education and Science of the Russian Federation for financial support within grant No. 0778-2020-0005.

Acknowledgments: Technical support by the SPbSU X-ray Diffraction and 'Geomodel' Resource Centers is gratefully acknowledged. There are two anonymous reviewers are thanked for fruitful remarks and corrections.

Conflicts of Interest: The authors declare no conflict of interest.

References

1. Chukanov, N.V.; Pekov, I.V.; Rastsvetaeva, R.K. Crystal chemistry, properties and synthesis of microporous silicates containing transition elements. *Russ. Chem. Rev.* **2004**, *73*, 205–223. [CrossRef]
2. Ferreira, P.; Ferreira, A.; Rocha, J.; Soares, M.R. Synthesis and Structural Characterization of Zirconium Silicates. *Chem. Mater.* **2001**, *13*, 355–363. [CrossRef]
3. Chukanov, N.V.V.; Pekov, I.V. Heterosilicates with Tetrahedral-Octahedral Frameworks: Mineralogical and Crystal-Chemical Aspects. *Rev. Mineral. Geochem.* **2005**, *57*, 105–143. [CrossRef]

4. Ilyushin, G.D.; Dem'yanets, L.N.; Ilyukhin, V.V.; Belov, N.V. Crystallization analougs of minerals and synthetic phases in the hydrotermal system $NaOH–ZrO_2–SiO_2–H_2O$. *Dokl. Akad. Nauk SSSR* **1983**, *271*, 1133–1136. (In Russian)
5. Ilyushin, G.D. Crystallization in the Na_2CO_3-ZrO_2–SiO_2–H_2O system at 450 °C and 0.1–0.05 GPa. *Inorg. Mater.* **2002**, *38*, 1249–1257. (In Russian)
6. Ilyushin, G.D. Hydrotermal crystallization in the system $NaOH–ZrO_2–SiO_2–H_2O$ at 450 °C: Phase relations $Na_4Zr_2Si_5O_{16} \cdot H_2O$, $Na_8ZrSi_6O_{18}$, $Na_3HZrSi_2O_8$, $Na_4Zr_2Si_3O_{12}$. *J. Inorg. Chem.* **2003**, *48*, 1002–1011. (In Russian)
7. Bortun, A.I.; Bortun, L.N.; Clearfield, A. Hydrothermal Synthesis of Sodium Zirconium Silicates and Characterization of Their Properties. *Chem. Mater.* **1997**, *9*, 1854–1864. [CrossRef]
8. Jale, S.R.; Ojo, A.; Fitch, F.R. Synthesis of microporous zirconosilicates containing ZrO_6 octahedra and SiO4 tetrahedra. *Chem. Commun.* **1999**, 411–412. [CrossRef]
9. Poojary, D.M.; Bortun, A.I.; Bortun, L.N.; Clearfield, A. Syntheses and X-ray Powder Structures of $K_2(ZrSi_3O_9)\cdot H_2O$ and Its Ion-Exchanged Phases with Na and Cs. *Inorg. Chem.* **1997**, *36*, 3072–3079. [CrossRef] [PubMed]
10. Cheetham, A.K.; Férey, G.; Loiseau, T. Open-Framework Inorganic Materials. *Angew. Chemie Int. Ed.* **1999**, *38*, 3268–3292. [CrossRef]
11. Gerasimovskii, V.I. Keldyshite—A new mineral. *Dokl. Akad. Nauk SSSR* **1962**, *142*, 916–918. (In Russian)
12. Khomyakov, A.P.; Kazakova, M.E.; Voronkov, A.A. New data on keldyshite, Doklady Akademii Nauk SSSR. *Dokl. Akad. Nauk SSSR* **1969**, *189*, 166–168. (In Russian)
13. Khomyakov, A.P.; Kazakova, M.E.; Vlasova, E.V.; Smolyaninova, N.N. Investigation on minerals of the keldyshite group. *Tr. Mineral. Muzeya Fersman Akad. Nauk SSSR* **1975**, *24*, 120–131. (In Russian)
14. Khomyakov, A.P. Types of regular intergrowths of minerals of the keldyshite group. *Geochemistry. Mineral. Intern. Geol. Congr. XXV Sess. Dokl. Owls. Geol. M* **1976**, *25*, 233–240. (In Russian)
15. Khomyakov, A.P. Parakeldyshite a new mineral. *Dokl. Akad. Nauk SSSR* **1977**, *237*, 703–705. (In Russian)
16. Khomyakov, A.P. Keldyshite group minerals. *Priroda* **2011**, *12*, 35–39. (In Russian)
17. Voronkov, A.A.; Shumyatskaya, N.G.; Pyatenko, Y.A. Crystal structure of a new natural modification of $Na_2Zr[Si_2O_7]$. *J. Struct. Chem.* **1970**, *11*, 866–867. (In Russian) [CrossRef]
18. Sizova, R.G.; Kuz'min, E.A.; Ilyukhin, V.V. Deciphering the continuous Patterson function of the Na,Zr-diorthosilicate $Na_2ZrSi_2O_7$ (parakeldyshite) by the vector subsystem method. *Konstitutsiya Svoistva Miner.* **1975**, *9*, 10–12. (In Russian)
19. Khalilov, A.D.; Khomyakov, A.P.; Makhmudov, S.A. Crystal structure of keldyshite $Na_2[Si_2O_6OH]$. *Dokl. Akad. Nauk SSSR* **1978**, *238*, 573–575. (In Russian)
20. Khomyakov, A.P.; Semenov, E.I.; Es'kova, E.M.; Voronkov, A.A. Kazakovite—A new mineral of the lovozerite group. *Zap. RMO* **1974**, *103*, 342–345. (In Russian)
21. Khomyakov, A.P. New data on mineralogy of lovozerite group. *Dokl. Akad. Nauk SSSR* **1977**, *237*, 199–202. (In Russian)
22. Khomyakov, A.P. *Mineralogy of Ultraagpaitic Alkaline Rocks*; Nauka: Moscow, Russia, 1990. (In Russian)
23. Khomyakov, A.P. Typomorphism of minerals of ultraagpaitic pegmatites. In *Scientific Foundations and Practical Use of Mineral Typomorphism*; Nauka: Moscow, Russia, 1980; pp. 152–157. (In Russian)
24. Khomyakov, A.P.; Yushkin, N.P. The principle of inheritance in crystallogenesis. *Dokl. Akad. Nauk SSSR* **1981**, *256*, 1229–1233. (In Russian)
25. Khomyakov, A.P. Ultraagpaite rocks of the Khibino-Lovozersky complex as an inexhaustible source minerals with unique properties. In *Fersman Scientific Session*; KSC Press: Apatity, Russia, 2007; pp. 202–205. (In Russian)
26. Yushkin, N.P.; Khomyakov, A.P.; Evzikova, N.Z. *The Principle of Inheritance in Mineralogenesis*; Nauka: Syktyvkar, Russia, 1984. (In Russian)
27. Pekov, I.V.; Zubkova, N.V.; Pushcharovsky, D.Y.; Kolich, U.; Tillmanns, E. Refined crystal structure of parakeldyshite and genetic crystal chemistry of zirconium minerals with diortho Si_2O_7 groups. *Kristallografiya* **2007**, *52*, 1100–1105. (In Russian)
28. Nikolova, R.P.; Fujiwara, K.; Nakayama, N.; Kostov-Kytin, V. Crystal structure of a new small-pore zirconosilicate $Na_2ZrSi_2O_7\cdot H_2O$ and its relation to stoichiometrically and topologically similar compounds. *Solid State Sci.* **2009**, *11*, 382–388. [CrossRef]

29. Chelishchev, N.F.; Khomyakov, A.P.; Berenshtein, B.G. Author's certificate AS No. 1096794 dated 02/08/1984 "Method for cleaning gases from sulfur dioxide". *Bul. Discov. Invent.* **1984**, *21*, 1–20. (In Russian)
30. Ilyushin, G.D.; Dem'yanets, L.N. Crystal structural features of ion transport in new OD-structures: Catapleiite $Na_2ZrSi_3O_9$ $2H_2O$ and hilairite $Na_2ZrSi_3O_9$ $3H_2O$. *Kristallografiya* **1988**, *33*, 383–387. (In Russian)
31. Zubkova, N.V.; Pekov, I.V.; Turchkova, A.G.; Pushcharovsky, D.Y.; Merlino, S.; Pazero, M.; Chukanov, N.V. Crystal structures of potassium-substituted forms of catapleiite and hilairite. *Kristallografiya* **2007**, *52*, 68–72. (In Russian)
32. Zubkova, N.V.; Ksenofontov, D.A.; Chukanov, N.V.; Pekov, I.V.; Artamonova, A.A.; Koshlyakova, N.N.; Bychkov, A.Y.; Pushcharovsky, D.Y. Crystal Chemistry of the Microporous Zirconosilicate $Na_6Zr_3[Si_9O_{27}]$, a Product of High-Temperature Transformation of Catapleiite, and Its Ag-Exchanged Form. *Minerals* **2020**, *10*, 243. [CrossRef]
33. Blatov, V.A.; Shevchenko, A.P.; Proserpio, D.M. Applied Topological Analysis of Crystal Structures with the Program Package ToposPro. *Cryst. Growth Des.* **2014**, *14*, 3576–3586. [CrossRef]
34. Anurova, N.A.; Blatov, V.A.; Ilyushin, G.D.; Blatova, O.A.; Ivanovschitz, A.; Dem'yanets, L.N. Migration maps of Li+ cations in oxygen-containing compounds. *Solid State Ionics* **2008**, *179*, 2248–2254. [CrossRef]
35. *Agilent Technologies CrysAlis CCD and CrysAlis RED*; Oxford Diffr. Ltd.: Yarnton, UK, 2014.
36. Sheldrick, G.M. Crystal structure refinement with SHELXL. *Acta Crystallogr. Sect. C Struct. Chem.* **2015**, *71*, 3–8. [CrossRef]
37. Eremin, R.A.; Kabanova, N.A.; Morkhova, Y.A.; Golov, A.A.; Blatov, V.A. High-throughput search for potential potassium ion conductors: A combination of geometrical-topological and density functional theory approaches. *Solid State Ionics* **2018**, *326*, 188–199. [CrossRef]
38. Fedotov, S.S.; Kabanova, N.A.; Kabanov, A.A.; Blatov, V.A.; Khasanova, N.R.; Antipov, E.V. Crystallochemical tools in the search for cathode materials of rechargeable Na-ion batteries and analysis of their transport properties. *Solid State Ionics* **2018**, *314*, 129–140. [CrossRef]
39. Meutzner, F.; Münchgesang, W.; Kabanova, N.A.; Zschornak, M.; Leisegang, T.; Blatov, V.A.; Meyer, D.C. On the Way to New Possible Na-Ion Conductors: The Voronoi-Dirichlet Approach, Data Mining and Symmetry Considerations in Ternary Na Oxides. *Chem. A Eur. J.* **2015**, *21*, 16601–16608. [CrossRef]
40. Ilyushin, G.D.; Blatov, V.A. Crystal chemistry of zirconosilicates and their analogs: Topological classification of MT frameworks and suprapolyhedral invariants. *Acta Crystallogr. Sect. B Struct. Sci.* **2002**, *58*, 198–218. [CrossRef] [PubMed]
41. Blatov, V.A.; O'Keeffe, M.; Proserpio, D.M. Vertex-, face-, point-, Schläfli-, and Delaney-symbols in nets, polyhedra and tilings: Recommended terminology. *CrystEngComm* **2010**, *12*, 44–48. [CrossRef]
42. Blatov, V.A. Methods for topological analysis of atomic networks. *J. Struct. Chem.* **2009**, *50*, 160–167.
43. Blatova, O.A.; Golov, A.A.; Blatov, V.A. Natural tilings and free space in zeolites: Models, statistics, correlations, prediction. *Z. Krist. Cryst. Mater.* **2019**, *234*, 421–436. [CrossRef]
44. Chong, S.; Aksenov, S.M.; Dal Bo, F.; Perry, S.N.; Dimakopoulou, F.; Burns, P.C. Framework Polymorphism and Modular Crystal Structures of Uranyl Vanadates of Divalent Cations: Synthesis and Characterization of $M(UO_2)(V_2O_7)$ (M = Ca,Sr) and $Sr_3(UO_2)(V_2O_7)_2$. *Z. Anorg. Allg. Chem.* **2019**, *645*, 981–987. [CrossRef]
45. Aksenov, S.M.; Chukanov, N.V.; Pekov, I.V.; Rastsvetaeva, R.K.; Hixon, A.E. Crystal structure and topological features of manganonaujakasite, a mineral with microporous heteropolyhedral framework related to AlPO-25 (ATV). *Microporous Mesoporous Mater.* **2019**, *279*, 128–132. [CrossRef]
46. Aksenov, S.M.; Mackley, S.A.; Deyneko, D.V.; Taroev, V.K.; Tauson, V.L.; Rastsvetaeva, R.K.; Burns, P.C. Crystal chemistry of compounds with lanthanide based microporous heteropolyhedral frameworks: Synthesis, crystal structures, and luminescence properties of novel potassium cerium and erbium silicates. *Microporous Mesoporous Mater.* **2019**, *284*, 25–35. [CrossRef]
47. Blatov, V.A.; Delgado-Friedrichs, O.; O'Keeffe, M.; Proserpio, D.M. Three-periodic nets and tilings: Natural tilings for nets. *Acta Crystallogr. Sect. A Found. Crystallogr.* **2007**, *63*, 418–425. [CrossRef]
48. Baur, W.H. The geometry of polyhedral distortions. Predictive relationships for the phosphate group. *Acta Crystallogr. Sect. B Struct. Crystallogr. Cryst. Chem.* **1974**, *30*, 1195–1215. [CrossRef]
49. Chernov, A.N.; Maksimov, V.A.; Ilyukhin, V.V.; Belov, N.V. Crystalline structure of monoclinic modification of K,Zr-diorthosilicate ($K_2ZrSi_2O_7$). *Sov. Phys. Dokl.* **1971**, *15*, 711–713. (In Russian)
50. Pertierra, P.; Salvado, M.A.; Garcia-Granda, S.; Trabajo, C.; Garcia, J.R.; Bortun, A.I.; Clearfield, A. Synthesis, Characterization, and X-Ray Powder Structure of $K_2ZrGe_2O_7$. *J. Solid State Chem.* **1999**, *148*, 41–49. [CrossRef]

51. Faggiani, R.; Crispin, C. Crystal structure of CaK, AsrO, and GdK_2P,0. *Can. J. Chem.* **1976**, *54*, 3319–3324. [CrossRef]
52. Leclaire, A.; Benmoussa, A.; Borel, M.M.; Grandin, A.; Raveau, B. Two forms of sodium titanium(III) diphosphate: α-$NaTiP_2O_7$ closely related to β-cristobalite and β-$NaTiP_2O_7$ isotypic with $NaFeP_2O_7$. *J. Solid State Chem.* **1988**, *77*, 299–305. [CrossRef]
53. Fleet, M.E.; Henderson, G.S. Sodium trisilicate: A new high-pressure silicate structure. *Phys. Chem. Miner.* **1995**, *22*, 383–386. [CrossRef]
54. Hamady, A.; Zid, M.F.; Jouini, T. Structure cristalline de KYP_2O_7. *J. Solid State Chem.* **1994**, *113*, 120–124. [CrossRef]
55. Muller-Buschbaum, H.K.; Rutter, I. A New Structure on Barium Lanthanoid Aluminates: $Ba_6Dy_2Al_4O_{15}$. *Z. Anorg. Allg. Chem.* **1989**, *573*, 89–94.
56. Poojary, D.M.; Borade, R.B.; Campbell, F.L.; Clearfield, A. Crystal Structure of Silicon Pyrophosphate (Form I) from Powder Diffraction Data. *J. Solid State Chem.* **1994**, *112*, 106–112. [CrossRef]
57. Newnham, R.E.; Redman, M.J.; Santoro, R.P. Crystal Structure of Yttrium and Other Rare-Earth Borates. *J. Am. Ceram. Soc.* **1963**, *46*, 253–256. [CrossRef]
58. Skshat, S.M.; Simonov, V.; Belov, N.V. Crystal structure of the synthetic sodium-scandium silicate $Na_3Sc(Si_2O_7)$. *Dokl. Akad. Nauk SSSR* **1969**, *184*, 337–340.
59. Lafuente, B.; Downs, R.T.; Yang, H.; Stone, N. The power of databases: The RRUFF project. In *Highlights in Mineralogical Crystallography*; Walter de Gruyter GmbH: Berlin, Germany, 2015; pp. 1–30. [CrossRef]
60. Sitarz, M.; Mozgawa, W.; Handke, M. Vibrational spectra of complex ring silicate anions—Method of recognition. *J. Mol. Struct.* **1997**, *404*, 193–197. [CrossRef]
61. Frost, R.L.; Bouzaid, J.M.; Martens, W.N.; Reddy, B.J. Raman spectroscopy of the borosilicate mineral ferroaxinite. *J. Raman Spectrosc.* **2007**, *38*, 135–141. [CrossRef]
62. Kirkpatrick, R.J.; Yarger, J.L.; McMillan, P.F.; Ping, Y.; Cong, X. Raman spectroscopy of C-S-H, tobermorite, and jennite. *Adv. Cem. Based Mater.* **1997**, *5*, 93–99. [CrossRef]
63. Yadav, A.K.; Singh, P. A review of the structures of oxide glasses by Raman spectroscopy. *RSC Adv.* **2015**, *5*, 67583–67609. [CrossRef]
64. Yakovenchuk, V.N.; Pakhomovsky, Y.A.; Konopleva, N.G.; Panikorovskii, T.L.; Bazai, A.; Mikhailova, J.A.; Bocharov, V.N.; Ivanyuk, G.Y.; Krivovichev, S.V. Batagayite, $CaZn_2(Zn,Cu)_6(PO_4)_4(PO_3OH)_3{\cdot}12H_2O$, a new phosphate mineral from Këster tin deposit (Yakutia, Russia): Occurrence and crystal structure. *Mineral. Petrol.* **2018**, *112*, 591–601. [CrossRef]
65. Khomyakov, A.P. *Mineralogy of Hyperagpaitic Alkaline Rocks*; Clarendon Press: Oxford, UK, 1995.
66. Krivovichev, S.V. Structural complexity of minerals: Information storage and processing in the mineral world. *Mineral. Mag.* **2013**, *77*, 275–326. [CrossRef]
67. Zolotarev, A.A.J.; Krivovichev, S.V.; Panikorovskii, T.L.; Gurzhiy, V.V.; Bocharov, V.N.; Rassomakhin, M.A. Dmisteinbergite, $CaAl_2Si_2O_8$, a Metastable Polymorph of Anorthite: Crystal-Structure and Raman Spectroscopic Study of the Holotype Specimen. *Minerals* **2019**, *9*, 570. [CrossRef]

Publisher's Note: MDPI stays neutral with regard to jurisdictional claims in published maps and institutional affiliations.

© 2020 by the authors. Licensee MDPI, Basel, Switzerland. This article is an open access article distributed under the terms and conditions of the Creative Commons Attribution (CC BY) license (http://creativecommons.org/licenses/by/4.0/).